

Circular Magnetization Processes In CoFeNi Electroplated Wires

H. García-Miquel ^{1,a}, V.M. García-Chocano ^{1,b}, G.V. Kurlyandskaya ^{2,c}

¹ Dpto. Ing. Electrónica, E.T.S.I.T., Universidad Politécnica de Valencia, Camino de Vera, s/n, 46022 Valencia, Spain.

² Ural State University named under A.M.Gorky , Dept. Magnetism and Magnetic Nanomaterials, Lenin Ave. 51, 620083, Ekaterinburg, Russian Federation.

^a hgmiquel@eln.upv.es, ^b vicgarch@aaa.upv.es, ^c galina@we.lc.ehu.es

Keywords: electroplated wire, circular magnetization, circular magnetic bistability.

Abstract. Circular magnetization processes in electroplated wires is an important topic having straight connection with sensor applications of these soft magnetic materials. In present work the longitudinal and circular hysteresis loops were measured and corresponding magnetization processes were studied in $\text{Cu}_{98}\text{Be}_2/\text{Co}_{16}\text{Fe}_{20}\text{Ni}_{64}$ wires. The longitudinal hysteresis loops, M_z - H_z , were measured by inductive technique in a frequency range of 10 to 70 Hz. The circular magnetization curves (M_ϕ - H_ϕ) were measured for frequencies of 50 and 100 kHz in the H_ϕ field up to 1500 A/m for different values of the axial external field of 0 to 500 A/m. The longitudinal and circular magnetization curves are comparatively analyzed.

1. Introduction

Composite wires consisting of highly conductive cylindric central part and a ferromagnetic cover layer were actively studied in recent years [1-4]. Although many interesting physical phenomenon like magnetic bistability, linear and non-linear magnetoimpedance were successfully investigated in such soft magnetic materials some of the research topics up to now were not sufficiently developed. Among them one could mention the dynamics of the domain wall displacement during the magnetization reversal or circular magnetization processes in bistable composite wires. For rapidly quenched wires some difficulties of the determination of M_ϕ - H_ϕ curves are caused by inhomogeneity of the H_ϕ field created by the flowing current [5-7]. In electroplated wires the changes of this field over the thickness of the magnetic layer can be neglected. For example, this simplification was used in a model description of giant magnetoimpedance in electroplated wires with high order magnetic anisotropy [8].

In this work the longitudinal and circular hysteresis loops were measured and corresponding magnetization processes were studied in $\text{Cu}_{98}\text{Be}_2/\text{Co}_{16}\text{Fe}_{20}\text{Ni}_{64}$ wires.

2. Experimental

$\text{Cu}_{98}\text{Be}_2/\text{Co}_{16}\text{Fe}_{20}\text{Ni}_{64}$ composite wires were obtained by electrodeposition technique. The diameter of non-magnetic CuBe was 60 μm and CoFeNi magnetic layer was 1 μm thick. The thickness of the magnetic layer was calculated through the deposition time and additionally checked by scanning electron microscopy, SEM (Fig.1). The length of the wires used for all measurements was 1.5 cm. The inner part composed of $\text{Cu}_{98}\text{Be}_2$ had a resistivity of $\rho_1 = 4\mu\Omega\cdot\text{cm}$ while outer part was composed of $\text{Co}_{16}\text{Fe}_{20}\text{Ni}_{64}$ layer with $\rho_2 = 15\mu\Omega\cdot\text{cm}$. The longitudinal hysteresis loops, M_z - H_z , were measured by inductive technique in a frequency range of 10 to 70 Hz. For measurements of circular magnetization curves an experimental set-up similar to that one described by A. Hernando et al [6] was used. Highly conductive (thermo- and electrically) silver paint was used for contacts preparation.

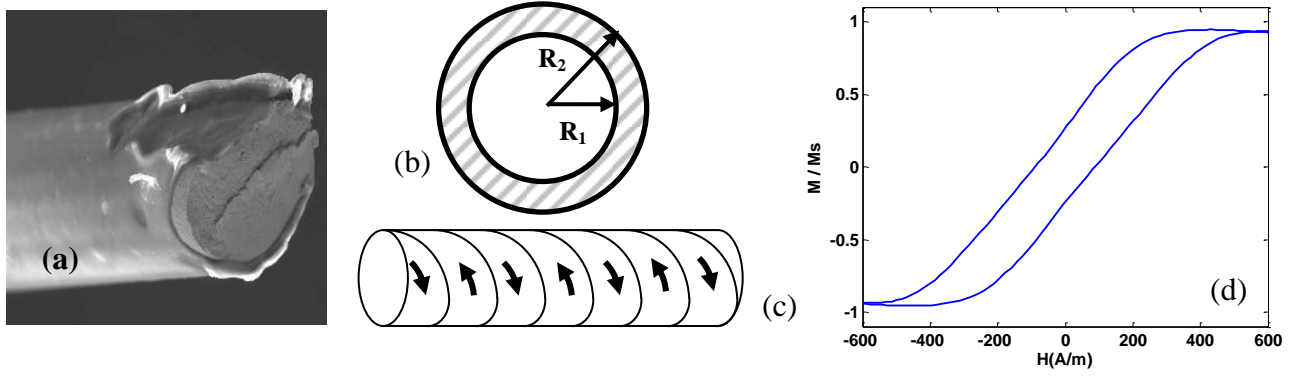


Figure 1: Electroplated wire of $\text{Cu}_{98}\text{Be}_2/\text{Co}_{16}\text{Fe}_{20}\text{Ni}_{64}$: (a) SEM image; (b) geometry: $R_1 = 60 \mu\text{m}$, $R_2 = 61 \mu\text{m}$; (c) inclined circular magnetic domains; and (d) axial hysteresis loop.

The circular magnetization curves (M_ϕ - H_ϕ) were obtained for frequencies of 50 and 100 kHz in the circular field, H_ϕ , up to 1500 A/m for different values of the axial external constant magnetic field, H , of 0 to 500 A/m. The axial external static magnetic field was created by Helmholtz coils.

3. Model description

Circular magnetization measurement technique was based on an acquire of voltages generated at the ends of the wire by a circumferential magnetic field. This field is simply created by an ac current flowing through the wire. The main problem of the modelization is caused by non-uniform distribution of a magnetic field inside the conductor (see model by A. Hernando et al [6] for the case of rapidly quenched wire). However, the geometry of electroplated wires is appropriate to consider the value of the field, H_ϕ , to be almost constant inside the interval of $R_1 < r < R_2$. For an infinite wire with its axis parallel to the Z coordinate axis and applying the cylindrical symmetry conditions to Maxwell equations one can deduce E_z , (the electrical field in Z direction) and M_ϕ , (the circular magnetization component):

$$E_z = \mu_0 \frac{\partial M_\phi}{\partial t} (r - R_2) \quad (1)$$

For E_z component related only to a circular magnetization.

Finally induced voltage observed along the wire can be expressed as $V_z = L \langle E_z \rangle$ where $\langle E_z \rangle$ correspond to the average electrical field between the limits of the ferromagnetic layer and L to the wire length. The induced voltage was measured and after its integration a value proportional to the sample magnetization M_ϕ was obtained. The magnetic field H_ϕ (considered constant) was deduced from the current by Ampere's law. Because of the different resistivities ρ_1 and ρ_2 in each part of the wire section, current distribution was not totally uniform, being greater in the centre comparing to the external ferromagnetic layer.

The current distribution can be modelled by equivalent circuit consisting of two parallel resistances with ρ_1/S_1 and ρ_2/S_2 Ω/m , where S_1 and S_2 are the respective section areas, with two currents I_1 and I_2 whose sum corresponds to the experimentally measured current, I . Applying this model the circular magnetic field for $[R_1 < r < R_2]$ it can be determined the H_ϕ by Eq. (2).

$$H_\phi = \frac{I}{2\pi r} \frac{R_1^2 \rho_2 + (r^2 - R_1^2) \rho_1}{R_1^2 \rho_2 + (R_2^2 - R_1^2) \rho_1}, \quad (2)$$

where I is the alternating current flowing through the wire. Skin depth is much larger than the tube thickness in case of frequency range under consideration. Therefore the skin effect is small can be

ignored in the calculations. On the other hand, axial magnetization processes have been studied using the conventional inductive method. The axial hysteresis loop is shown in Fig. 1(d).

Circular magnetization curves were measured with the circuit shown in Fig.2. The current can be obtained as $I = (V_1 - V_2)/R$. Fig.3 shows the shape of the voltage waveforms induced in the wire. The voltage along the wire, V_2 , contains both a sinusoidal component due to the wire impedance and the induced voltage peaks associated with circular magnetization process. By subtracting the sinusoidal voltage, one can get the peak of induced voltage associated with circular magnetization process $V_w = V_2 - I \cdot R_w$ (Fig.3), being R_w the resistance of the electroplated wire. Using the procedure of the integration of the peak voltage the circular hysteresis loop can be obtained (Fig.4).

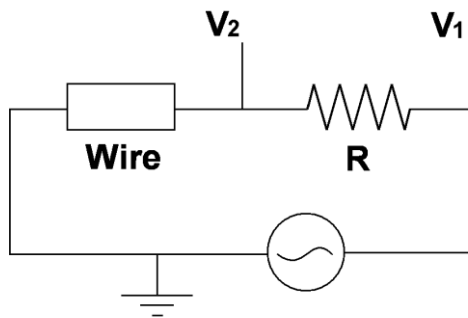


Figure 2: Circular magnetization measurement circuit.

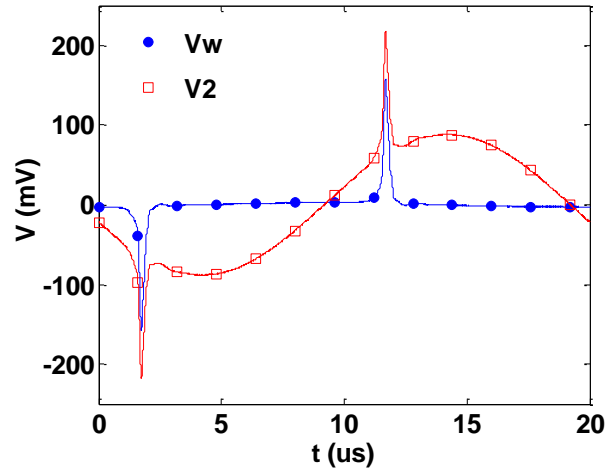


Figure 3: Magnetization-induced voltage, V_w , and total voltage, V_2 , in the wire.

3. Results and conclusions

Fig. 1 (d) shows axial hysteresis loop of electroplated wire measured for the frequency of 30 Hz. The hysteresis loops shows the presence of the transverse anisotropy component. Generally, it can be circumferential or radial [9]. It is logical to suppose, that the easy magnetization axis is nearly circumferential due to the influence of a circumferential magnetic field which appears during the fabrication of the samples, so as the shape anisotropy.

In order to describe the magnetic softness of the samples the standard characteristic, coercive field, H_c , was obtained from the hysteresis loop. For the frequency $f = 30$ Hz the coercive field $H_c = 100$ A/m. The shape of the hysteresis loop is quite complex, giving ground to assume non-single domain structures in these wires. Both longitudinal magnetic bistability, i.e. magnetization process consisting of a large Barkhausen jump and quick propagation of single domain wall and circular magnetic bistability are interesting phenomena employed for technological applications and magnetization dynamic studies [2, 9-11]. At the same time experimental data on bistable behaviour in electroplated wires are very limited [12].

Circular hysteresis loops were obtained from voltages induced in the wire for different values of axial external static magnetic field. As shown in Fig.4, the circular magnetic quasi bistable behaviour is clearly seen for small axial fields. Although longitudinal magnetic bistability for electroplated wires was reported in 2001 [12], the circular magnetic bistability was not yet observed in such materials. An increase of the value of the axial field resulted in the changes of the parameters of M_ϕ - H_ϕ loops with decrease and disappearance of the square shape of the loop for axial fields above 200 A/m. The summary of the analysis of the shape of M_ϕ - H_ϕ loops is shown in Fig.4. The remanent magnetization and coercive fields are represented as function of the axial

external magnetic field. The frequency of the alternating current was not an important parameter for the frequencies

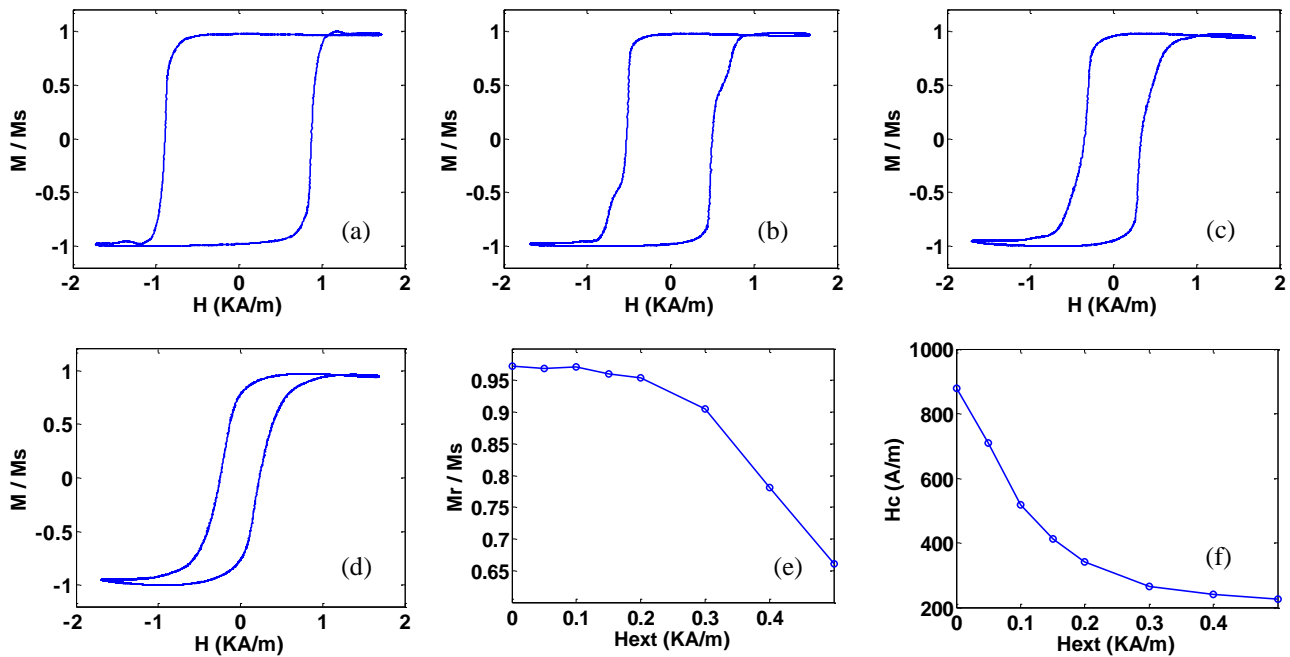


Figure 4: M_ϕ - H_ϕ curve at 50kHz for axial fields to the sample of (a) 0 A/m, (b) 100 A/m, (c) 200 A/m and (d) 400 A/m, (e) circular remanent magnetization as a function of the axial field, (f) coercitive fields collected from the circular hysteresis loops measured for different values of axial magnetic field.

under consideration. The slope for the variation of the circular magnetic field, H_ϕ , was the important factor because the amplitude of the voltage induced along the wire was the function of the time for the circular field, as can be seen from the Eq.(1). Most probably the domain structure of the $\text{Cu}_{98}\text{Be}_2/\text{Co}_{16}\text{Fe}_{20}\text{Ni}_{64}$ wires consisted in the inclined circular magnetic domains.

In conclusion, longitudinal and circular hysteresis loops were measured and corresponding magnetization processes were studied in $\text{Cu}_{98}\text{Be}_2/\text{Co}_{16}\text{Fe}_{20}\text{Ni}_{64}$ wires. Circular hysteresis loops were quasi bistable in a small external axial field but the remanence for corresponding axial hysteresis loops was non-zero. With an increase of the static axial field, both the remanent magnetizations and the coercive fields obtained from the circular hysteresis loops were decreased and the bistable behaviour disappeared.

4. References

- [1] R.S. Beach, N. Smith, C.L. Platt, F. Jeffers, A.E. Berkowitz, *Appl. Phys. Lett.* 68 (1996) 2753.
- [2] G.V. Kuryandskaya, H. García-Miquel, M. Vazquez, A.V. Svalov, V.O. Vaskovskiy, *J. Magn. Magn. Mater.*, 242-245 (2002) 291.
- [3] A.S. Antonov, N.A. Buznikov, I.T. Iakubov, A.N. Lagarkov, A.L. Rakhmanov, *J. Phys. D: Appl. Phys.* 34 (2001) 752.
- [4] H. García-Miquel, G.V. Kuryandskaya, V.I. Levit, *J. Magn. Magn. Mater.*, 300 (2006) e55.
- [5] K. Mohri, L.V. Panina, T. Uchiyama, K. Bushida, M. Noda, *IEEE Trans. Magn.*, 31 (1995) 1266.
- [6] A. Hernando, J.M. Barandiaran, *J. Phys. D.: Appl. Phys.*, 11 (1978) 1539.
- [7] D.-X. Chen, A. Hernando, L. Pascual, *Meas. Sci. Tech.*, 15 (2004) 365.
- [8] G.V. Kuryandskaya, H. Yakabchuk, E. Kisker, N.G. Bebenin, H. García-Miquel, M. Vázquez, V.O. Vaskovskiy, *J. Appl. Phys.* 90 (2001) 6280.
- [9] M. Vazquez, A. Hernando, *J. Phys. D* 29 (1996) 939.
- [10] M. Vazquez, C. Gomez-Polo, *J. Kor. Phys. Soc* 31 (1997) 471.
- [11] A. Chizhik, J. Gonzalez, A. Zhukov, J. M. Blanco, *J. Phys. D: Appl. Phys.* 36 (2003) 419.
- [12] G.V. Kuryandskaya, H. Garcia-Miquel, A.V. Svalov, V.O. Vaskovsky, M. Vazquez, *Physics of Metals and Metallography* 91 (2001) S139.